Influence of limestone mineral addition in cements on the efficacy of SCMs in mitigating alkali-silica reaction assessed by accelerated mortar bar test

Marie Joshua Tapas Ph.D.
School of Civil and Environmental Engineering, University of Technology Sydney
81 Broadway Ultimo, NSW 2007 Australia
Corresponding author: mariejoshua.tapas@uts.edu.au

Kirk Vessalas Ph.D.
School of Civil and Environmental Engineering, University of Technology Sydney
81 Broadway Ultimo, NSW 2007 Australia
Email: kirk.vessalas@uts.edu.au

Paul Thomas Ph.D.
School of Mathematical and Physical Sciences, University of Technology Sydney
81 Broadway Ultimo, NSW 2007 Australia
Email: paul.thomas@uts.edu.au

Prof. Vute Sirivivatnanon Ph.D.
School of Civil and Environmental Engineering, University of Technology Sydney
81 Broadway Ultimo, NSW 2007 Australia
Email: vute.sirivivatnanon@uts.edu.au

Abstract

This study evaluates the effect of limestone mineral addition in cement on the efficacy of supplementary cementitious materials (SCMs) in mitigating alkali-silica reaction (ASR) using the accelerated mortar bar test (AMBT). Mortars with and without SCMs were prepared by substituting portion of 0% limestone GP cement with increasing amounts of limestone. Mortars with SCMs (25% fly ash or 65% slag) exhibit negligible expansion regardless of the limestone content in the binder while mortars without SCMs exhibit high and almost identical expansion for all limestone substitutions. The expansion results show that limestone does not aggravate ASR, has no detrimental effect on the efficacy of SCMs in ASR mitigation and likewise has no observable ASR mitigating properties under the test conditions. The calcium silicate hydrate (C-S-H) composition is not affected by the amount of limestone which suggests that limestone has no influence on the alkali uptake in the C-S-H. This is supported by the pore solution analysis results where SCMs (both fly ash and slag) have drastically reduced the pore solution alkali concentration over time, whereas, limestone substitution only resulted to alkali

reduction equivalent to substitution (dilution). Moreover, the carboaluminate phases formed when limestone is present were observed to decompose under AMBT conditions and thus, their influence on ASR mitigation is not possible to discern from this study.

Keywords: alkali-silica reaction; fly ash; slag; limestone; carboaluminates

Introduction

Cement production results in substantial amount of carbon dioxide (CO_2) emissions. Calcination of limestone in order to produce cement clinker accounts for about 60% of CO_2 emissions at a cement plant (Scrivener, John and Gartner, 2016). Addition of supplementary cementitious materials (SCMs), such as in the case of blended cements, has the potential to reduce the economic and environmental impact of cement-based construction materials. Most commonly used SCMs, fly ash and slag, are however industrial by-products and increasingly becoming scarce resources (Scrivener, John and Gartner, 2016).

The foreseen shortage of fly ash supply is fueled by the closure of coal-fired power plants in various parts of the world in favour of renewable sources of energy (Johnson and Chau, 2019, Nalbandian-Sugden, 2015). Australia is no exception with around one-third of its coal-fired power stations closed during 2012-2017, with remaining expected to close as well in the coming decades (Burke, Best and Jotzo, 2018). Coal-fired power stations pollute the environment heavily due to significant production of greenhouse gases that can lead to global warming (ECRC, 2017, Thomson, Huelsman and Ong, 2018). Increasing recycling of steel and introduction of more efficient steelmaking technologies also lowers the availability of slag. Currently, slag production is only about 5-10% of total cement production worldwide and is expected to further decrease in the coming years (Scrivener, Martirena, Bishnoi and Maity, 2018). Thus, there is a need to explore alternative materials for blending into cement.

Limestone is an abundant natural resource and its addition to cement offers a potential route to reducing the CO_2 emissions associated with cement production through partial substitution. General Purpose (GP) cement is

69 the most common commercially used cement in Australia and accounts for over 85% of the total cement market
70 for production of concrete (Mohammadi and South, 2016). The current allowable mineral addition in the
71 Australian Standard AS 3972 for Type GP cement is 7.5%. Due to the potential environmental benefits of
72 increased limestone addition, there is a drive to increase limestone content in Australian GP cement from 7.5%
73 to 12% (Mohammadi and South, 2016). Whereas, the effect of limestone on various properties of concrete has
74 been widely investigated (Lollini, Redaelli and Bertolini, 2014, Mohammadi and South, 2016, Schmidt,
75 Lothenbach, Romer, Neuenschwander and Scrivener, 2009, Tsivilis, Batis, Chaniotakis, Grigoriadis and
76 Theodossis, 2000, Tsivilis, Tsantilas, Kakali, Chaniotakis and Sakellariou, 2003), its effect on the alkali-silica
77 reaction (ASR) and on the efficacy of SCMs in mitigating ASR is still not fully understood.
78
79 ASR is a major durability issue and can occur in concrete if three factors are present: reactive silica in the
80 aggregate, highly alkaline pore solution, and sufficient moisture. High alkali content pore solution facilitates
81 dissolution of reactive silica phases in the aggregate. Dissolved silica in the pore solution then bind cations (Na^+,
82 K^+, and Ca^{2+}) to form the ASR product (alkali calcium silicate hydrate gel) which can induce pressure build up,
83 resulting in expansion, and eventual cracking of the concrete (Chatterji, 2005, Rajabipour, Giannini, Dunant,
84 Ideker and Thomas, 2015).
85
86 The available literature on the effect of limestone addition on ASR is, however, limited and in disagreement.
87 Limestone has been variously reported to have either no effect on ASR acting as an inert diluent (Tennis, Thomas
88 and Weiss, 2011, Thomas, Delagrave, Blair and Barcelo, 2013) or to aid in ASR mitigation (Hooton, Nokken and
89 Thomas, 2007, Rajbhandari, 2010). At the extreme, limestone has been reported to mitigate ASR more
90 effectively than Class F fly ash (Turk, Kina and Bagdiken, 2017), while synergistic effects of limestone with fly ash
91 have also been recently reported to result in better ASR mitigating properties (Wang, Wu and Mei, 2019),
92 although, in the latter case the elevated SiO_2 content of the limestone powder (15.71%) may have played a role
93 in mitigation. Purity of the limestone used is, therefore, critical in ensuring that mitigation observed in laboratory
94 studies is due to the limestone and not other constituents. The Australian standard, for instance, requires only
95 75% $CaCO_3$ content in minerals to meet the criteria as suitable limestone mineral addition (AS 3972).
96

The reported ability of limestone to mitigate ASR is largely attributed to cement dilution (Hooton, Nokken and Thomas, 2007, Rajbhandari, 2010), to limestone providing additional sites for nucleation resulting in microstructural densification (Arora, Sant and Neithalath, 2016, Matschei, Lothenbach and Glasser, 2007, Ramezanianpour and Hooton, 2014), and to the formation of monocarboaluminates when limestone is present in cement (Chen and Yang, 2013). Calcite ($CaCO_3$) present in limestone reacts with aluminate phases in the cement to form monocarboaluminates resulting in a denser microstructure and an increase in compressive strength (Bonavetti, Donza, Menendez, Cabrera and Irassar, 2003, Bonavetti, Rahhal and Irassar, 2001, Tennis, Thomas and Weiss, 2011, Thomas, Delagrave, Blair and Barcelo, 2013, Voglis, Kakali, Chaniotakis and Tsivilis, 2005). The reaction is limited, however, by the amount of alumina available to react with calcite and above a certain replacement level, excess limestone (calcite) may result in degradation of concrete properties (Ramezanianpour and Hooton, 2014, Scrivener, Martirena, Bishnoi and Maity, 2018). Excess limestone in cement acts as a diluent and therefore limestone replacements greater than 15% has been reported to result in reduction in strength (Dhir, Limbachiya, McCarthy and Chaipanich, 2007).

Given the relative uncertainty of the role of limestone in ASR mitigation, this study investigates the influence of limestone on the reactivity of a reactive aggregate and on the efficacy of SCMs in mitigating ASR using the accelerated mortar bar test (AMBT), AS 1141.60.1. The Australian test method AS 1141.60.1 was shown to be a relatively good test method for classifying “slowly reactive” and “reactive” aggregates consistent with field performance (Sirivivatnanon, Mohammadi and South, 2016). The effect of limestone mineral addition and AMBT test conditions on the microstructure and composition of mortars and pastes are also investigated.

Materials and Methods

Raw Materials

All raw materials (cement, aggregate, SCMs, limestone) used in this study were sourced in Australia. The cement, limestone and SCMs were supplied by Cement Australia and the reactive greywacke aggregate was supplied by Cement Concrete and Aggregates Australia (CCAA), the peak body for the heavy construction

materials industry in Australia. Oxide compositions of cements, SCMs, limestone and aggregate utilized in the study are shown in Table 1. The XRF equipment used was PHILIPS PW2400 XRF Rh end-window tube coupled with "SUPERQ" software. The total alkali content of the cement conventionally calculated as equivalent sodium oxide [$\%Na_2O_{eq} = \%Na_2O + (0.658 \times \%K_2O)$] is 0.54% Na_2O_{eq} which is less than the 0.60% Na_2O_{eq} cement alkali limit specified for Australian cements. Both fly ash and slag conform to Australian specifications, AS/NZS 3582.1 and AS 3582.2 respectively. Table 2 shows the mineralogical composition of reactive aggregate greywacke as determined by petrographic analysis. The petrographic examination was conducted in accordance with Australian Standards AS2758.1 (1985) and ASTM C-295 (1990) by the Department of Geology, University of Newcastle, Australia.

The ground limestone (GL) used in this study was shown to be predominantly calcite ($CaCO_3$) by XRD with trace proportions of quartz also present (Fig. 1). XRD was carried out using a Bruker D8 Discover XRD. Diffraction patterns were collected in Bragg-Brentano mode using Cu Kα radiation (1.5418 Å) in the range 5 to 70° 2θ using a step size 0.04 °/second. Phases were identified using the ICDD PDF 4+ database.

The GL and GP cement were characterised by thermogravimetric analysis (TG) using TA Instruments SDT-Q600 Simultaneous TGA/DSC. The analysis was performed in a nitrogen atmosphere, by heating from 23 °C to 1000 °C and at a heating rate of 10 °C/min. The weight loss curves obtained are shown in Fig. 2. The mineral-addition-free GP cement showed only 0.2% mass loss between 600-800 °C confirming the negligible amount of $CaCO_3$ present. The GL, on the other hand, registered a mass loss of about 43%, which indicates that it is 98% $CaCO_3$. This is consistent with 43% loss of ignition (LOI) in Table 1 which corresponds to the release of carbon dioxide (CO_2) at higher temperatures.

Accelerated Mortar Bar Test (AMBT)

AMBT was conducted to evaluate the effect of substituting portion of the cement with limestone on ASR mitigation. Mortar bars composed of 1 part of cement to 2.25 parts of graded aggregate by mass (440 g cementitious materials per 990 g of aggregate, Table 3) and water to cementitious materials ratio equal to 0.47

by mass were prepared in accordance with AS 1141.60.1 (Standards Australia, 2014). Limestone substitution was carried out at 0%, 8%, 12% and 17% by mass of cement. The SCMs were used at the recommended replacement dosages: 25% fly ash and 65% slag (Standards Australia, 2015).

The specimens were prepared in 25 x 25 x 285 mm moulds with a gauge length of 250 mm then cured in ≥90% RH 23±2 °C for 24 hours. After, the specimens were carefully de-moulded and put in a container filled with water. The container was then placed in an oven set at 80 °C for another 24 hours to allow the specimens to further cure. After which, zero hour length measurements were obtained using a horizontal comparator prior immersing the specimens in 1M NaOH solution at 80 °C for 28 days. The mortar specimens were taken out of the storage solution at 1, 3, 7, 10, 14, 21, and 28 days for succeeding expansion measurements. The expansion limits of AS 1141.60.1 are listed in Table 4. The reliability of the Australian test method is discussed in the study of Sirivivatnanon et al. (Sirivivatnanon, Mohammadi and South, 2016).

Analysis of ASR Gel and C-S-H Composition

The mortar specimens were sectioned post-AMBT (after 28 days) to characterize the calcium silicate hydrate (C-S-H) and ASR gel composition. The mortar was cut using diamond saw (about 2mm thickness) and then immersed in isopropanol for 5 days to remove free water (solvent exchange process) and prevent further reactions. The samples were then stored in a vacuum desiccator to prevent carbonation until analysed.

Polished sections were prepared for SEM-EDS analysis by subjecting the cut mortar sections to resin vacuum impregnation and polishing. Manual polishing was first carried out to ensure the surface is flat and remove any extra resin on the surface of the sample using sandpaper grades 500 and 1200 respectively. This was followed by automated polishing using MD Largo Struers discs lubricated with petrol and diamond spray as a polishing agent (9µm, 3µm and 1µm particle sizes). After polishing, the samples were subjected to 2 minutes ultrasonic cleaning to remove polishing debris and then stored in a vacuum desiccator for at least 2 days to dry. All analysed samples were carbon-coated to prevent charging during SEM imaging.

Imaging and elemental analysis were carried out using FEI Quanta 200 SEM fitted with a Bruker XFlash 4030 EDS detector. Imaging was carried out in backscattered electron (BSE) mode with a 15 kV accelerating voltage and 12.5 mm working distance. To ensure consistent beam current, X-ray intensities from copper film placed on the metallic sample holder was measured before each measurement to obtain a target "system factor" by adjusting the spot size. A predefined list of elements (O, Na, Mg, Al, Si, P, S, Cl, K, Ca, Ti, Fe) was used for identification and quantification. The composition of C-S-H was measured by point EDS analysis on the hydration rims around the hydrated clinker to minimize intermixing with other phases. Minimum of 200 points were analysed per sample. The technique was based on the method of Rossen and Scrivener (Rossen and Scrivener, 2017).

Pore Solution Analysis of Blended Pastes

In order to investigate the effect of limestone, fly ash and slag on the pore solution alkali concentration, blended pastes with 25% replacement levels of the cementitious materials were prepared in sealed containers (200ml) at water to cementitious materials ratio of 0.47. The sealed containers were stored in a temperature and humidity cabinet at ≥90% RH, 23±2 °C. Pore solution extractions were carried out at 28 days and 168 days using a compression testing machine and a force of 1000kN. All extracted solutions were filtered using a 0.2µm membrane to remove solids and after which analysed using inductively coupled plasma optical emission spectroscopy (ICP-OES). ICP-OES analysis was carried out using Shimadzu ICPE-9000.

Formation of carboaluminate phases and the effect of AMBT conditions on stability

In order to show the effect of limestone on the phases (i.e. demonstrate the formation of carboaluminates in different paste systems when limestone is present) as well as determine the effect of AMBT conditions on the stability of carboaluminates, two sets of limestone blended pastes with mix composition based on the mortar test specimens (i.e. same cement, limestone, SCM and water proportions), were prepared in 50 x 50 x 50 mm moulds using an electric hand mixer and left to cure inside a temperature and humidity cabinet at ≥90% RH, 23±2 °C for 1 day. After 1 day curing, the blended pastes were demoulded and whereas, one set was left to age

at ≥90% RH, 23±2 °C in the same temperature and humidity cabinet, the other set was subjected to AMBT conditions (1M NaOH 80 °C) similar to the mortar bars.

The limestone blended pastes were taken out at 21 days and 56 days for phase and microstructural characterization using XRD and SEM. No drying technique was employed to preserve the integrity of the phases to optimum quality. The solvent exchange method using isopropanol, although generally accepted as the best method to arrest hydration, still affects the amount of hydrates (ettringite crystals, AFm, carboaluminates) (Snellings, Chwast, Cizer, Belie, Dhandapani, Durdzinski, Elsen, Haufe, Hooton, Patapy, Santhanam, Scrivener, Snoeck, Steger, Tongbo, Vollpracht, Winnefeld and Lothenbach, 2018). For XRD, the samples were analysed the same day they were taken out from storage. The blended pastes were powdered using mortar and pestle and then carefully loaded into the XRD sample holders, ensuring to not over press the surface to prevent preferred orientation. XRD patterns were obtained using Bruker D8 Discover XRD in Bragg-Brentano mode using Cu Kα radiation (1.5418 Å) from 5 to 70 °2θ at a scan rate of 0.04 °/second. Phases were identified using the ICDD PDF 4+ database. To characterize the microstructure, the blended pastes were fractured for secondary electron (SE) SEM imaging. Similar to the XRD samples, hydration was not deliberately stopped for the SEM samples in order to minimize damage to the microstructure. The samples were also "fractured" only right before SEM imaging to lessen the possibility of carbonation. The "fractured surface" samples with size maximum of approximately 5 x 5 mm (LxW) were directly mounted on metal stubs using carbon tape and coated with gold-palladium prior to SEM imaging to prevent charging. SEM imaging was carried out using Zeiss Supra 55VP SEM. Images were collected at 15 kV accelerating voltage and 12.5 mm working distance.

Results and Discussions

AMBT Expansion Results

AMBT expansion results in Fig. 3 show all mortars without SCM exhibiting high degree of expansion. Mortars containing SCMs (25%FA or 65%SL) show negligible expansion regardless of limestone substitution. Thus, the increase in limestone substitution does not influence the efficacy of SCMs in mitigation. Each point in the AMBT

plot represents an average of 3 samples and as the error is too small (≤0.01%), it is no longer reported as error bars. The AMBT expansion results are consistent with the work of Thomas et al. (Thomas, Delagrave, Blair and Barcelo, 2013) which showed that the expansion levels for Portland cement and Portland-limestone cement mixtures (12% limestone addition) are almost identical for mixtures with the same type of SCM and replacement level and that the efficacy of cement replacement with Class F fly ash or slag cement does not appear to be influenced by the presence of 12% limestone in the cement. The expansion limits of 0.10 at 10 days and 0.3% at 21 days are based on AS 1141.60.1 which is the Australian standard for testing aggregate reactivity typically extended for assessing SCM efficacy (Sirivivatnanon, Hocking, Cheney and Rocker, 2019, Sirivivatnanon, Mohammadi and South, 2016). Australia, at present, has no dedicated standard for assessing SCM efficacy.

Adding SCMs (25%FA or 65%SL) reduced the expansion to negligible levels independently of the limestone content. Thus, limestone has no detrimental effect on the ability of SCMs to mitigate ASR. The ability of SCMs to mitigate ASR has been widely investigated (Bickmore, Nagy, Gray and Brinkerhoff, 2006, Chappex and Scrivener, 2012, Chappex and Scrivener, 2013, Duchesne and Berube, 1994, Durand, Berard, Roux and Soles, 1990, Hong and Glasser, 1999, Kim, Olek and Jeong, 2015, Shafaatian, Akhavan, Maraghechi and Rajabipour, 2013, Thomas, 2013). The mitigating properties of SCMs are reported to be due to: 1) the products formed by SCM reactions resulting in microstructure densification and lower permeability, thereby retarding alkali ingress (Shafaatian, Akhavan, Maraghechi and Rajabipour, 2013), 2) modification of the calcium silicate hydrate (C-S-H) composition resulting in enhanced alkali binding capacity (Duchesne and Berube, 1994, Durand, Berard, Roux and Soles, 1990, Hong and Glasser, 1999, Kim, Olek and Jeong, 2015, Thomas, 2013) and 3) aluminium present in SCMs such as fly ash and slag suppressing ASR by inhibiting dissolution of reactive silica in aggregates (Bickmore, Nagy, Gray and Brinkerhoff, 2006, Chappex and Scrivener, 2012, Chappex and Scrivener, 2013).

Fig. 4 illustrates clearly that mortars with limestone and no SCM exhibit almost similar expansion regardless of the limestone content in the binder (0 to 17%GL). The observed nearly identical degree of expansion with increasing limestone content in mortars without SCMs suggests that whereas limestone ($CaCO_3$) does not aggravate ASR, under the conditions present during AMBT, limestone also appears to have no observable ASR mitigating properties. Whereas, cement limestone substitution is expected to result in reduced pore solution alkali concentration, the effect of alkali dilution is not visible in the AMBT expansion plots and this is likely

because the 1M NaOH storage solution is dominating the pore solution of the mortars. Limestone also reportedly densifies the microstructure due to the formation of monocarboaluminates (Bonavetti, Rahhal and Irassar, 2001, Chen and Yang, 2013). The expansion results however suggest that it does not appear to contribute to ASR mitigation under the test conditions.

Characterization of the Mortar Specimens Post-AMBT

Fig. 5 shows the SEM images of cross-sectioned greywacke mortar specimens without SCM addition post 28 days AMBT (0%GL, 8%GL, 12%GL and 17%GL). Extensive cracking can be observed in all mortars which is consistent with the high degree of expansion during AMBT. High magnification image of the ASR gel in the mortar with 12%GL but no SCM shown in Fig. 5e appears similar to that reported in literature (Andreas Leemann, 2017, Fernandes, 2009, Leemann and Lothenbach, 2008). The gel is sandwiched between an aggregate particle that appears to have cracked and fully separated.

Table 3 tabulates corresponding EDS point locations 1 to 5 in Fig. 5e which shows that the ASR gel contains a significant amount of calcium (Ca), silicon (Si), and sodium (Na). Si concentration in the ASR gel dominates at an average of 64%, with notable concentrations of Ca and Na at approximately 17%. Negligible amount of potassium (about 1%) detected is consistent with other ASR gel studies in AMBT specimens (Gavrilenko, Amo, Perez and Garcia, 2007, Shafaatian, Akhavan, Maraghechi and Rajabipour, 2013). In contrast, ASR gel in concretes that underwent either concrete prism test or taken from structures damaged by ASR typically contain almost equivalent contents of Na and K (Andreas Leemann, 2017, Leemann, Katayama, Fernandes and Broekmans, 2016, Leemann and Merz, 2013, Thaulow, Jakobsen and Clark, 1996). The obtained average Ca/Si ratio and (Na+K)/Si ratio of the ASR gel is 0.26 and 0.29 respectively, which closely agrees with that reported in other studies (Andreas Leemann, 2017, Leemann, Katayama, Fernandes and Broekmans, 2016, Leemann and Merz, 2013, Thaulow, Jakobsen and Clark, 1996).

299 The negligible concentration of potassium (K) in the gel indicates that the 1M NaOH storage solution is masking
300 the available potassium in the pore solution of mortars without SCMs. This finding is consistent with the study
301 of Golmakani and Hooton (Golmakani and Hooton, 2019) which reported that AMBT mortar bar pore solutions
302 showed mainly sodium, with hardly any potassium. Likewise, this also supports the nearly identical expansion
303 observed regardless of limestone substitution amount in mortars without SCMs. Due to the high alkali
304 concentration of the 1M NaOH storage solution, the dilution effect resulting from increasing levels of limestone
305 substitution is not possible to detect by AMBT, confirming that AMBT is not a suitable method for assessing the
306 effect of cement dilution (due to limestone substitution) on ASR and, hence, the influence of limestone content
307 on ASR gel composition was not further investigated.
308
309
310 Fig. 6 shows the low magnification SEM images of the cross-sectioned greywacke AMBT specimens with SCM
311 contents at recommended replacement levels: 0%GL+25%FA, 0%GL+65%SL, 17%GL+25%FA and 17%GL+65%SL.
312 The mortar specimens show no major cracking in the aggregate or paste which is consistent with negligible levels
313 of expansion during AMBT. This result supports the high efficacy of SCMs in ASR mitigation independent of the
314 amount of limestone present in the mortar. Minor cracks observed are likely due to the cutting process.
315
316 Some of the mortar specimens were subjected to SEM-EDS analysis post-AMBT to investigate the effect of
317 limestone addition on C-S-H composition. Mortars without limestone (0%GL) and with maximum limestone
318 content (17%GL) were chosen to better illustrate the effect of limestone. The EDS scatter plots in Fig. 7 show
319 that the Si/Ca and Al/Si ratio of the C-S-H is comparable in mortars without SCMs for both 0%GL and 17%GL.
320 This agrees with the studies of C-S-H composition in ambient cured limestone blended cement pastes (Adu-
321 Amankwah, Zajac, Stabler, Lothenbach and Black, 2017, Weerdt, Haha, Saout, Kjellsen, Justnes and Lothenbach,
322 2011). Adu-Amankwah et al. (Adu-Amankwah, Zajac, Stabler, Lothenbach and Black, 2017) reported that there
323 was no observed significant change in the C-S-H Al/Si ratio with increasing limestone content. Likewise, it has
324 been shown that the Ca/Si ratio and Al/Si ratio of OPC and OPC-limestone blended pastes are similar and
325 constant over time (Weerdt, Haha, Saout, Kjellsen, Justnes and Lothenbach, 2011).
326 Fig. 7 also shows that adding 25%FA or 65%SL increases the Si/Ca and Al/Si ratio of the C-S-H. For the same
327 amount of SCM, the effect on C-S-H composition is comparable regardless of limestone content in the binder.

328 The results therefore demonstrate that although the SCMs affect the C-S-H composition, it is independent of
329 the amount of limestone present. The modification in C-S-H composition when SCMs are present is linked to
330 increased alkali binding capacity in the C-S-H (Chappex and Scrivener, 2012, Hong and Glasser, 2002, L'Hôpital,
331 Lothenbach, Scrivener and D.A.Kulik, 2016). Since C-S-H composition affects the ability to adsorb alkali (i.e.
332 higher Si/Ca ratio, higher ability to bind alkali), comparable C-S-H composition for 0%GL and 17%GL mortars
333 (without SCM or with SCM but same type and dosage) suggests that limestone content has no effect on the alkali
334 binding capacity of the C-S-H. EDS spot analysis was carried out to investigate the effect of Si/Ca ratio on the
335 alkali binding capacity of the C-S-H, however, the values obtained for the alkali contents of the C-S-H were too
336 small to determine variation and are not reported. Nevertheless, the result of pore solution analysis of blended
337 pastes in Fig. 8 demonstrates the effect of limestone, fly ash and slag replacement on pore solution alkali
338 concentration.
339
340 Extracted pore solutions of blended pastes at 28 days and 168 days with equivalent replacement level (25%) of
341 cementitious materials (fly ash, slag and limestone) are shown in Fig. 8. The results show much lower alkali
342 concentration in all pastes when SCMs are present and the reduction of total alkali (Na and K) is a function of
343 the type of SCM. Fly ash clearly reduces the pore solution alkali concentration more than slag which is consistent
344 with another study (Canham, Page and Nixon, 1987). Since 25% SCM replacement does not have an identical
345 effect on the pore solution alkali concentration, this indicates that the effect of SCM addition is more than just
346 cement dilution. A similar trend was also observed for pore solutions extracted after 168 days (6 months). The
347 strong pozzolanic reaction associated with higher amount of reactive silica in fly ash increases the amount of C-
348 S-H formed with lower Ca/Si ratio that are able to take up more alkalis. Further decrease in alkali concentration
349 with time is also clearly observed. This indicates that the process of alkali binding is continuous with time as the
350 SCM reacts in the paste.
351
352 Fig.8 also clearly demonstrates alkali dilution induced by 25% limestone substitution. The decrease in the
353 concentration of alkali cations with limestone substitution is consistent with that reported in another study
354 where 50% limestone substitution resulted to 50% reduction in Na and K concentration (Schöler, Lothenbach,
355 Winnefeld, Haha, Zajac and Ludwig, 2017).This indicates that limestone only dilutes cement and therefore has

no capacity to continuously bind alkalis unlike SCMs which showed decrease in alkali concentration as a function of time. Moreover, a slight increase in the concentration of alkalis from 28 days to 168 days can be observed in both OPC and OPC-limestone blend with time consistent with what has been reported in several studies (Lothenbach, Saout, Gallucci and Scrivener, 2008, Vollpracht, Lothenbach, Snellings and Haufe, 2016, Weerdt, Haha, Saout, Kjellsen, Justnes and Lothenbach, 2011). Although part of the alkalis is bound in the C-S-H, the alkali concentration increases with time as alkalis continue to be released during the hydration of clinkers and as the volume of the liquid phase present decreases (Lothenbach, Saout, Gallucci and Scrivener, 2008).

Effect of AMBT conditions on carboaluminates (blended cement pastes)

XRD patterns in Figs. 9 and 10 confirm the formation of carboaluminates as well as the presence of ettringite crystals in the limestone blended cement pastes cured and aged in a temperature and humidity cabinet at ≥90%RH, 23±2 °C. Carboaluminates were not observed in cement pastes without limestone as expected. Fig. 9 shows that monocarboaluminate is the main carbonate phase present in cement-limestone pastes at age 21 and 56 days. The interest on 21 days is due to the test limits of AS 1141.60.1 (0.3% expansion at 21 days). The curing was further extended to 56 days to determine the influence of age on the carboaluminate phases. A tiny peak due to the presence of hemicarboaluminate in cement-limestone pastes that is present at 21 days is observed to have disappeared at 56 days. This indicates that whereas, hemicarboaluminates form at early hydration, they slowly convert to the more stable monocarboaluminates over time as more carbonate ions become available in the pore solution (Adu-Amankwah, Zajac, Stabler, Lothenbach and Black, 2017, Ipavec, Gabrovgek, Vuk, Kaucic, Macek and Medenz, 2011). Formation of carboaluminates results in increased amount of hydrates and also indirectly stabilises ettringite leading to a decrease in porosity and more dense microstructure (Lothenbach, Saout, Gallucci and Scrivener, 2008). Formed ettringite slowly converts to monosulfoaluminate when there is insufficient gypsum in the system. When $CaCO_3$ is present, monosulfoaluminate-monocarboaluminate transformation occurs, thereby providing new source of additional sulfate ions in the system resulting in the re-precipitation of ettringite (Bonavetti, Rahhal and Irassar, 2001).

Fig. 10 shows the XRD patterns of cement-fly ash-limestone and cement-slag-limestone blends at 21 days. Hemicarboaluminate was observed as the main carbonate phase in the cement-slag-limestone blends, whereas, monocarboaluminate is the dominant carbonate phase in the cement-fly ash-limestone blends similar to that of plain cement. The difference in the dominant carbonate phase in blends with either fly ash or slag is consistent with that reported in previous studies (Adu-Amankwah, Zajac, Stabler, Lothenbach and Black, 2017, Weerdt, Haha, Saout, Kjellsen, Justnes and Lothenbach, 2011). It is possible that the high substitution levels of slag at 65% increased the aluminium sufficiently to favour the presence of hemicarboaluminate over monocarboaluminate. It has been reported that when the availability of aluminate is much higher than the availability of carbonate, hemicarboaluminate tends to be more stable (Ipavec, Gabrovgek, Vuk, Kaucic, Macek and Medenz, 2011, Whittaker, Zajac, Ben Haha, Bullerjahn and Black, 2014).

Fig. 11 show the effect of AMBT conditions on the limestone blended cement pastes at 21 and 56 days. In all cases, regardless of the presence or absence of SCMs, ettringite and carboaluminate peaks disappear which indicates that both phases are unstable under the test conditions. It is well established that ettringite is intrinsically unstable in cement pastes above 70 °C (Scrivener and Taylor, 1993, Shimada and Young, 2004, Taylor, Famy and Scrivener, 2001). Monocarboaluminates, on the other hand, are reported to be stable at temperatures ≤ 70 °C, but decompose at temperatures ≥ 90 °C (Matschei, Lothenbach and Glasser, 2007). This is in close agreement with the current study which clearly shows that carboaluminates decompose when exposed to 1M NaOH 80 °C.

SEM images in Fig. 12 are in agreement with the observations from XRD. Whereas, the SEM images of the limestone blended cement pastes after 21 days at ≥90%RH 23±2 °C show presence of ettringite crystals (needle-like morphology), the limestone blended pastes post 21 days exposure to 1M NaOH 80 °C confirm absence of ettringite crystals. SEM and XRD results therefore indicate that since AMBT conditions facilitate the decomposition of ettringite crystals and carboaluminates, their influence on ASR mitigation is not possible to assess using AMBT.

Conclusions

The accelerated mortar bar test (AMBT) expansion results show that limestone mineral addition up to 17% in cement has no detrimental effect on the ability of SCMs to mitigate ASR. The substitution of cement with either 25% fly ash or 65% slag showed sufficient capacity of the SCM to mitigate ASR regardless of limestone content in the binder. AMBT mortars without SCM show nearly identical levels of expansion regardless of limestone content in the binder which indicates that whereas limestone does not aggravate ASR, it also does not actively mitigate ASR like SCMs.

SEM-EDS analysis of the C-S-H phases in the mortars post-AMBT show that limestone does not modify the C-S-H composition. The increase in Si/Ca and Al/Si ratio of the C-S-H that occurs when SCMs are present results in better alkali uptake. Pore solution analysis of blended cement pastes with SCMs and limestone support this findings. The pore solution alkali concentration when SCMs are present continuously decreases over time whereas limestone substitution merely results in dilution. Limestone addition, therefore, does not change the alkali binding capacity of the C-S-H and therefore does not actively reduce the pore solution concentration like SCMs.

The ASR gel observed in the mortar without SCM is primarily composed of sodium, silicon and calcium. The negligible presence of potassium in the ASR gel indicates that the 1M NaOH storage solution dominates the pore solution of the mortar. This indicates that AMBT is not a suitable method to assess the effect of alkali dilution, an expected effect of cement limestone substitution, due to the high concentrations of alkali available from the bath. Further, although carboaluminates were observed in ≥90%RH 23±2 °C cured limestone cement pastes (which confirms that limestone is not inert in the system), their absence in pastes cured under AMBT conditions (1M NaOH and 80 °C) indicate that these phases are unstable under these conditions and therefore do not contribute to microstructure densification. Thus, the influence of carboaluminates on ASR mitigation is not possible to assess by the AMBT method.

Whereas, the study shows that the efficacy of SCMs in mitigating ASR is not affected by the presence of limestone and therefore increasing cement limestone substitutions should have no negative effects for ASR

mitigation, it also clearly brings about the limitations of AMBT - which is its inability to assess the effect of cement dilution as well the influence of carboaluminates on ASR mitigation. In order to fully investigate the influence of limestone on ASR, CPT tests need to be carried out as under the CPT testing conditions the alkali content of the concrete is finite and storage temperature is much lower (38°C) which will inhibit dissolution of phases. Studies on the influence of limestone on ASR will be the subject of further investigation through CPT testing.

Data Availability Statement

Some or all data, models, or code that support the findings of this study are available from the corresponding author upon reasonable request.

Acknowledgements

This study is a part of University of Technology Sydney research funded through Australian Research Council Research Hub for Nanoscience Based Construction Materials Manufacturing (NANOCOMM) with the support of Cement Concrete and Aggregates Australia (CCAA). This work would also not have been possible without laboratory equipment provided by Laboratory of Construction Materials at EPFL Switzerland courtesy of Professor Karen Scrivener.

References

Adu-Amankwah, S., Zajac, M., Stabler, C., Lothenbach, B., and Black, L. (2017). "Influence of limestone on the hydration of ternary slag cements." *Cem. Concr. Res.*, 100, 96-109.http://dx.doi.org/10.1016/j.cemconres.2017.05.013

Andreas Leemann, T. K., Isabel Fernandes, Maarten A. T. M. Broekmans (2017). "Raman microscopy of alkali-silica reaction (ASR) products formed in concrete." *Cem. Concr. Res.*, 102, 41–47.http://dx.doi.org/10.1016/j.cemconres.2017.08.014

Arora, A., Sant, G., and Neithalath, N. (2016). "Ternary blends containing slag and interground/blended limestone: Hydration, strength, and pore structure." *Constr. Build. Mater.*, 102, 113–124.http://dx.doi.org/10.1016/j.conbuildmat.2015.10.179

Bickmore, B. R., Nagy, K. L., Gray, A. K., and Brinkerhoff, A. R. (2006). "The effect of $Al(OH)_4^-$ on the dissolution rate of quartz." *Geochim. Cosmochim. Acta*, 70, 290–305.https://doi.org/10.1016/j.gca.2005.09.017

Bonavetti, V., Donza, H., Menendez, G., Cabrera, O., and Irassar, E. F. (2003). "Limestone filler cement in low w/c concrete: A rational use of energy." *Cem. Concr. Res.*, 33 865–871.https://doi.org/10.1016/S0008-8846(02)01087-6

Bonavetti, V., Rahhal, V., and Irassar, E. (2001). "Studies on the carboaluminate formation in limestone-filler blended cements." *Cem. Concr. Res.*, 31, 853-859.https://doi.org/10.1016/S0008-8846(01)00491-4

Burke, P. J., Best, R., and Jotzo, F. (2018). "Closures of coal-fired power stations in Australia:Local unemployment effects." *CCEP Working Paper 1809*, Crawford School of Public Policy, The Australian National University.

Canham, I., Page, C. L., and Nixon, P. J. (1987). "Aspects of the Pore Solution Chemistry of Blended Cements Related to the Control of Alkali-Silica Reaction." *Cem. Concr. Res.*, 17, 839-844.https://doi.org/10.1016/0008-8846(87)90046-9

Chappex, T., and Scrivener, K. (2012). "Alkali fixation of C–S–H in blended cement pastes and its relation to alkali silica reaction." *Cem. Concr. Res.*, 42, 1049–1054.https://doi.org/10.1016/j.cemconres.2012.03.010

Chappex, T., and Scrivener, K. (2012). "The influence of aluminium on the dissolution of amorphous silica and its relation to alkali silica reaction." *Cem. Concr. Res.*, 42, 1645–1649.http://dx.doi.org/10.1016/j.cemconres.2012.09.009

Chappex, T., and Scrivener, K. (2013). "The Effect of Aluminum in Solution on the Dissolution of Amorphous Silica and its Relation to Cementitious Systems." *J. Am. Ceram. Soc.*, 96(2), 592-597. https://doi-org.ezproxy.lib.uts.edu.au/10.1111/jace.12098

Chatterji, S. (2005). "Chemistry of alkali–silica reaction and testing of aggregates." *Cem. Concr. Compos.*, 27, 788–795.https://doi.org/10.1016/j.cemconcomp.2005.03.005

Chen, C.-T., and Yang, W.-C. (2013). "Mitigation of Alkali-Silica Reaction in Mortar with Limestone Addition and Carbonation." *Third International Conference on Sustainable Construction Materials and Technologies*Japan.

498 Dhir, R. K., Limbachiya, M. C., McCarthy, M. J., and Chaipanich, A. (2007). "Evaluation of Portland limestone
499 cements for use in concrete construction." *Materials and Structures* 459-473.https://doi.org/10.1617/s11527-
500 006-9143-7
501 Duchesne, J., and Berube, M. A. (1994). "The Effectiveness of Supplementary Cementing Materials in
502 Suppressing Expansion Due to ASR: Another Look at the Reaction Mechanisms Part 2: Pore Solution
503 Chemistry." *Cem. Concr. Res.*, 24(2), 221-230.https://doi.org/10.1016/0008-8846(94)90047-7
504 Durand, B., Berard, J., Roux, R., and Soles, J. (1990). "Alkali-Silica Reaction: The Relation Between Pore
505 Solution Characteristics and Expansion Test Results." *Cem. Concr. Res.*, 20, 419-
506 428.https://doi.org/10.1016/0008-8846(90)90032-S
507 ECRC (2017). "Environment and Communications References Committee-Retirement of coal fired power
508 stations."
509 <https://www.aph.gov.au/Parliamentary_Business/Committees/Senate/Environment_and_Communications/C
510 oal_fired_power_stations/Final_Report>.
511 Fernandes, I. (2009). "Composition of alkali–silica reaction products at different locations within concrete
512 structures." *Mater. Charact.*, 60, 655-668.http://dx.doi.org/10.1016/j.matchar.2009.01.011
513 Gavrilenko, E., Amo, D. G. d., Perez, B. C., and Garcia, E. G. (2007). "Comparison of ASR-gels in concretes
514 against accelerated mortar bar test samples." *Mag. Concr. Res.*, 59(7), 483–494.https://doi-
515 org.ezproxy.lib.uts.edu.au/10.1680/macr.2007.59.7.483
516 Golmakani, F., and Hooton, R. D. (2019). "Impact of pore solution concentration on the accelerated mortar bar
517 alkali-silica reactivity test." *Cem. Concr. Res.*, 121, 72-80.https://doi.org/10.1016/j.cemconres.2019.02.008
518 Hong, S.-Y., and Glasser, F. P. (1999). "Alkali binding in cement pastes Part I. The C-S-H phase." *Cem. Concr.*
519 *Res.*, 29, 1893–1903.https://doi.org/10.1016/S0008-8846(99)00187-8
520 Hong, S.-Y., and Glasser, F. P. (2002). "Alkali sorption by C-S-H and C-A-S-H gels Part II. Role of alumina." *Cem.*
521 *Concr. Res.*, 32, 1101–1111.https://doi.org/10.1016/S0008-8846(02)00753-6
522 Hooton, R. D., Nokken, M., and Thomas, M. D. A. (2007). "Portland-Limestone Cement: State of the Art Report
523 and Gap Analysis For CSA A 3000." *University of Toronto*
524 Ipavec, A., Gabrovgek, R., Vuk, T., Kaucic, V., Macek, J., and Medenz, A. (2011). "Carboaluminate Phases
525 Formation During the Hydration of Calcite-Containing Portland Cement." *J. Am. Cer. Soc.*, 94(4), 1238-1242.
526 https://doi.org/10.1111/j.1551-2916.2010.04201.x

Johnson, S., and Chau, K. (2019). "More U.S. coal-fired power plants are decommissioning as retirements continue." *Today in Energy*, U.S. Energy Information Administration.

Kim, T., Olek, J., and Jeong, H. (2015). "Alkali–silica reaction: Kinetics of chemistry of pore solution and calcium hydroxide content in cementitious system." *Cem. Concr. Res.*, 71, 36–45.http://dx.doi.org/10.1016/j.cemconres.2015.01.017

L'Hôpital, E., Lothenbach, B., Scrivener, K., and D.A.Kulik (2016). "Alkali uptake in calcium alumina silicate hydrate (C-A-S-H)." *Cem. Concr. Res.*, 85, 122–136.http://dx.doi.org/10.1016/j.cemconres.2016.03.009

Leemann, A., Katayama, T., Fernandes, I., and Broekmans, M. A. T. M. (2016). "Types of alkali–aggregate reactions and the products formed." *Constr. Mater.*, 169, 128-135.http://dx.doi.org/10.1680/jcoma.15.00059

Leemann, A., and Lothenbach, B. (2008). "The influence of potassium–sodium ratio in cement on concrete expansion due to alkali-aggregate reaction." *Cem. Concr. Res.*, 38, 1162–1168.https://doi.org/10.1016/j.cemconres.2008.05.004

Leemann, A., and Merz, C. (2013). "An attempt to validate the ultra-accelerated microbar and the concrete performance test with the degree of AAR-induced damage observed in concrete structures." *Cem. Concr. Res.*, 49, 29–37.http://dx.doi.org/10.1016/j.cemconres.2013.03.014

Lollini, F., Redaelli, E., and Bertolini, L. (2014). "Effects of portland cement replacement with limestone on the properties of hardened concrete." *Cem. Concr. Compos.*, 46, 32–40.http://dx.doi.org/10.1016/j.cemconcomp.2013.10.016

Lothenbach, B., Saout, G. L., Gallucci, E., and Scrivener, K. (2008). "Influence of limestone on the hydration of Portland cements." *Cem. Concr. Res.*, 38, 848–860.https://doi.org/10.1016/j.cemconres.2008.01.002

Matschei, T., Lothenbach, B., and Glasser, F. P. (2007). "The role of calcium carbonate in cement hydration." *Cem. Concr. Res.*, 37(4), 551-558.https://doi.org/10.1016/j.cemconres.2006.10.013

Matschei, T., Lothenbach, B., and Glasser, F. P. (2007). "Thermodynamic properties of Portland cement hydrates in the system $CaO–Al_2O_3–SiO_2–CaSO_4–CaCO_3–H_2O$." *Cem. Concr. Res.*, 37, 1379–1410.https://doi.org/10.1016/j.cemconres.2007.06.002

Mohammadi, I., and South, W. (2016). "General purpose cement with increased limestone content in Australia." *ACI Mater. J.*, 113, 335-347.http://dx.doi.org/10.14359/51688703

554 Mohammadi, J., and South, W. (2016). "Effect of up to 12% substitution of clinker with limestone on
555 commercial grade concrete containing supplementary cementitious materials." *Constr. Build. Mater.*, 115,
556 555–564.http://dx.doi.org/10.1016/j.conbuildmat.2016.04.071
557 Nalbandian-Sugden, H. (2015). "New regulatory trends: effects on coal-fired powerplants and coal demand."
558 *CCC/262*.
559 Rajabipour, F., Giannini, E., Dunant, C., Ideker, J., and Thomas, M. (2015). "Alkali–silica reaction: Current
560 understanding of the reaction mechanisms and the knowledge gaps." *Cem. Concr. Res.*, 76, 130–
561 146.http://dx.doi.org/10.1016/j.cemconres.2015.05.024
562 Rajbhandari, N. (2010). "Determining the Effect of Intergrinding Limestone with Portland Cement on the
563 Durability of Concrete with and without SCM " Masters Thesis, The University of New Brunswick.
564 Ramezanianpour, A. M., and Hooton, R. D. (2014). "A study on hydration, compressive strength, and porosity
565 of Portland-limestone cement mixes containing SCMs." *Cem. Concr. Compos.*, 51, 1-
566 13.https://doi.org/10.1016/j.cemconcomp.2014.03.006
567 Rossen, J. E., and Scrivener, K. L. (2017). "Optimization of SEM-EDS to determine the C–A–S–H composition in
568 matured cement paste samples." *Mater. Charact.*, 123, 294-
569 306.https://doi.org/10.1016/j.matchar.2016.11.041
570 Schmidt, T., Lothenbach, B., Romer, M., Neuenschwander, J., and Scrivener, K. (2009). "Physical and
571 microstructural aspects of sulfate attack on ordinary and limestone blended Portland cements." *Cem. Concr.*
572 *Res.*, 39(12), 1111-1121.https://doi.org/10.1016/j.cemconres.2009.08.005
573 Schöler, A., Lothenbach, B., Winnefeld, F., Haha, M. B., Zajac, M., and Ludwig, H.-M. (2017). "Early hydration
574 of SCM-blended Portland cements: A pore solution and isothermal calorimetry study." *Cem. Concr. Res.*, 93,
575 71-82.https://doi.org/10.1016/j.cemconres.2016.11.013
576 Scrivener, K., Martirena, F., Bishnoi, S., and Maity, S. (2018). "Calcined clay limestone cements (LC3)." *Cem.*
577 *Concr. Res.*, 114, 49–56.https://doi.org/10.1016/j.cemconres.2017.08.017
578 Scrivener, K. L., John, V. M., and Gartner, E. M. (2016). "Eco-Efficient Cements: Potential, economically viable
579 solutions for a low CO_2 cement-based materials industry." United Nations Environment Program.
580 Scrivener, K. L., and Taylor, H. F. W. (1993). "Delayed ettringite formation: a microstructural and
581 microanalytical study." *Adv. Cem. Res.*, 5(20), 139 - 146.https://doi-
582 org.ezproxy.lib.uts.edu.au/10.1680/adcr.1993.5.20.139

583 Shafaatian, S. M. H., Akhavan, A., Maraghechi, H., and Rajabipour, F. (2013). "How does fly ash mitigate alkali–
584 silica reaction (ASR) in accelerated mortar bar test (ASTM C1567)?" *Cem. Concr. Compos.*, 37, 143–
585 153.https://doi.org/10.1016/j.cemconcomp.2012.11.004
586 Shimada, Y., and Young, J. F. (2004). "Thermal stability of ettringite in alkaline solutions at 80°C." *Cem. Concr.*
587 *Res.*, 34, 2261–2268.https://doi.org/10.1016/j.cemconres.2004.04.008
588 Sirivivatnanon, V., Hocking, D., Cheney, K., and Rocker, P. (2019). "Reliability of extending AS1141.60.1 and
589 60.2 test methods to determine ASR mitigation." *Concrete 2019, Concrete in Practice-Progress through*
590 *Knowledge* Sydney, Australia.
591 Sirivivatnanon, V., Mohammadi, J., and South, W. (2016). "Reliability of new Australian test methods in
592 predicting alkali silica reaction of field concrete." *Construction and Building Materials*, 126, 868-
593 874.https://doi.org/10.1016/j.conbuildmat.2016.09.055
594 Sirivivatnanon, V., Mohammadi, J., and South, W. (2016). "Reliability of new Australian test methods in
595 predicting alkali silica reaction of field concrete." *Constr. Build. Mater.*, 126 868–
596 874.http://dx.doi.org/10.1016/j.conbuildmat.2016.09.055
597 Snellings, R., Chwast, J., Cizer, O., Belie, N. D., Dhandapani, Y., Durdzinski, P., Elsen, J., Haufe, J., Hooton, D.,
598 Patapy, C. d., Santhanam, M., Scrivener, K., Snoeck, D., Steger, L., Tongbo, S., Vollpracht, A., Winnefeld, F., and
599 Lothenbach, B. (2018). "Report of TC 238-SCM: hydration stoppage methods for phase assemblage studies of
600 blended cements—results of a round robin test." *Mater. Struct.*, 51(111).https://doi.org/10.1617/s11527-018-
601 1237-5
602 Standards Australia (2014). "Methods for sampling and testing aggregates Method 60.1: Potential alkali-silica
603 reactivity—Accelerated mortar bar method." Standards Australia.
604 Standards Australia (2015). "Alkali Aggregate Reaction—Guidelines on Minimising the Risk of Damage to
605 Concrete Structures in Australia." SAI Global Limited, Sydney, Australia.
606 Taylor, H., Famy, C., and Scrivener, K. (2001). "Delayed Ettringite Formation." *Cem. Concr. Res.*, 31, 683-
607 693.https://doi.org/10.1016/S0008-8846(01)00466-5
608 Tennis, P. D., Thomas, M. D. A., and Weiss, W. J. (2011). "State-of-the-Art Report on Use of Limestone in
609 Cements of up to 15%." Portland Cement Association.

610 Thaulow, N., Jakobsen, U. H., and Clark, B. (1996). "Composition of Alkali Silica Gel and Ettringite in Concrete
611 Railroad Ties: SEM-EDX and X-Ray Diffraction Analyses." *Cem. Concr. Res.*, 26(2), 309-
612 318.https://doi.org/10.1016/0008-8846(95)00219-7
613 Thomas, M. D. A. (2013). *Supplementary Cementing Materials in Concrete*, Taylor & Francis Group, LLC, Boca
614 Raton, Florida.
615 Thomas, M. D. A., Delagrave, A., Blair, B., and Barcelo, L. (2013). "Equivalent Durability Performance of
616 Portland Limestone Cement." *Concr. Int.*, 39-35
617 Thomson, V. E., Huelsman, K., and Ong, D. (2018). "Coal-fired power plant regulatory rollback in the United
618 States: Implications for local and regional public health." *Energy Policy*, 123, 558–568
619 Tsivilis, S., Batis, G., Chaniotakis, E., Grigoriadis, G., and Theodossis, D. (2000). "Properties and behavior of
620 limestone cement concrete and mortar." *Cem. Concr. Res.*, 30(10), 1679-1683.https://doi.org/10.1016/S0008-
621 8846(00)00372-0
622 Tsivilis, S., Tsantilas, J., Kakali, G., Chaniotakis, E., and Sakellariou, A. (2003). "The permeability of Portland
623 limestone cement concrete." *Cem. Concr. Res.*, 33(9), 1465-1471.https://doi.org/10.1016/S0008-
624 8846(03)00092-9
625 Turk, K., Kina, C., and Bagdiken, M. (2017). "Use of binary and ternary cementitious blends of F-Class fly-ash
626 and limestone powder to mitigate alkali-silica reaction risk." *Constr. Build. Mater.*, 151, 422–
627 427.https://doi.org/10.1016/j.conbuildmat.2017.06.075
628 Voglis, N., Kakali, G., Chaniotakis, E., and Tsivilis, S. (2005). "Portland-limestone cements. Their properties and
629 hydration compared to those of other composite cements." *Cem. Concr. Compos.*, 27 191–
630 196.https://doi.org/10.1016/j.cemconcomp.2004.02.006
631 Vollpracht, A., Lothenbach, B., Snellings, R., and Haufe, J. (2016). "The pore solution of blended cements: a
632 review." *Mater. Struct.*, 49, 3341–3367
633 Wang, H., Wu, D., and Mei, Z. (2019). "Effect of fly ash and limestone powder on inhibiting alkali aggregate
634 reaction of concrete." *Constr. Build. Mater.*, 210, 620–626.https://doi.org/10.1016/j.conbuildmat.2019.03.219
635 Weerdt, K. D., Haha, M. B., Saout, G. L., Kjellsen, K. O., Justnes, H., and Lothenbach, B. (2011). "Hydration
636 mechanisms of ternary Portland cements containing limestone powder and fly ash." *Cem. Concr. Res.*, 41, 279–
637 291.http://dx.doi.org/10.1016/j.cemconres.2010.11.014

638 Whittaker, M., Zajac, M., Ben Haha, M., Bullerjahn, F., and Black, L. (2014). "The role of the alumina content of
639 slag, plus the presence of additional sulfate on the hydration and microstructure of Portland cement-slag
640 blends." *Cem. Concr. Res.*, 66, 91-101.https://doi.org/10.1016/j.cemconres.2014.07.018

641

642

643

644 **Table 1.** XRF Oxide Composition of the raw materials

Oxide wt.%	0% Limestone GP Cement (OPC)	Ground Limestone	Fly Ash	Slag	Greywacke
SiO_2	20.36	1.30	59.21	34.12	66.85
TiO_2	0.30	0.04	1.11	0.87	0.65
Al_2O_3	5.25	0.43	28.11	14.37	14.24
Fe_2O_3	3.06	0.21	3.68	0.30	3.80
Mn_3O_4	0.05	0.02	0.11	0.36	0.09
MgO	1.35	0.36	0.53	5.31	1.58
CaO	63.55	55.11	2.48	41.59	1.94
Na_2O	0.28	0.14	0.63	0.35	4.25
K_2O	0.40	0.06	1.18	0.26	3.11
P_2O_5	0.22	0.02	0.41	0.01	0.14
SO_3	2.44	0.02	0.16	2.83	0.19
Na_2O_{eq}	0.54	0.18	1.41	0.52	-
L.O.I.	2.77	42.99	1.05	0.35	2.29

645
646
647 **Table 2.** Greywacke Mineralogical Composition

Mineral	%
Microcrystalline feldspars	37
Microcrystalline Quartz	17
Quartz	13
Epidote	8
Moderately Strained Quartz	7
Feldspar	7
Lithic clasts	5
Calcite	3
Chlorite	2
Sericite	1

648

649 **Table 3.** AS 1141.60.1 aggregate grading requirements

Sieve size, mm		% by mass
Passing	Retained on	
4.75	2.36	10
2.36	1.18	25
1.18	0.60	25
0.60	0.30	25
0.30	0.15	15

650

651 **Table 4.** AS 1141.60.1 aggregate reactivity classification

Mean mortar bar expansion E, %		AS 1141.60.1 aggregate reactivity classification
Duration of specimens in 1M NaOH at 80 °C		
10 days	21 days	
-	E < 0.10	Non-reactive
E < 0.10	0.10 ≤ E < 0.30	Slowly reactive
E > 0.10	-	Reactive
-	0.30 ≤ E	Reactive

652

653

654 **Table 5.** Elemental Analysis of the ASR Gel (normalized without oxygen). Data are quoted in atom % (at%)

EDS Location	**at%**								
	Ca	**Al**	**Si**	**Na**	**K**	**Na+K**	**Ca/Si**	**(Na+K)/Si**	**Total**
ASR Gel Pt 1	14.59	1.20	65.27	18.48	0.45	18.93	0.22	0.29	100.00
ASR Gel Pt 2	19.29	0.70	61.46	17.41	1.13	18.55	0.31	0.30	100.00
ASR Gel Pt 3	18.88	0.79	62.86	16.19	1.28	17.47	0.30	0.28	100.00
ASR Gel Pt 4	16.87	1.55	66.63	13.30	1.65	14.95	0.25	0.22	100.00
ASR Gel Pt 5	14.67	1.16	62.02	21.72	0.43	22.15	0.24	0.36	100.00
Average	**16.86**	**1.08**	**63.65**	**17.42**	**0.99**	**18.41**	**0.26**	**0.29**	**100.00**
Minimum	**14.59**	**0.70**	**61.46**	**13.30**	**0.43**	**14.95**	**0.22**	**0.22**	**100.00**
Maximum	**19.29**	**1.55**	**66.63**	**21.72**	**1.65**	**22.15**	**0.31**	**0.36**	**100.00**

655

656

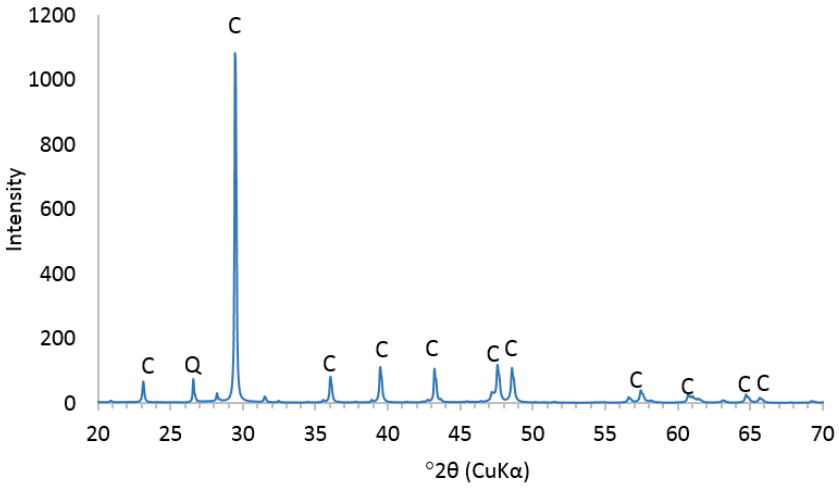

Fig.1. XRD pattern of ground limestone where C=calcite and Q=quartz

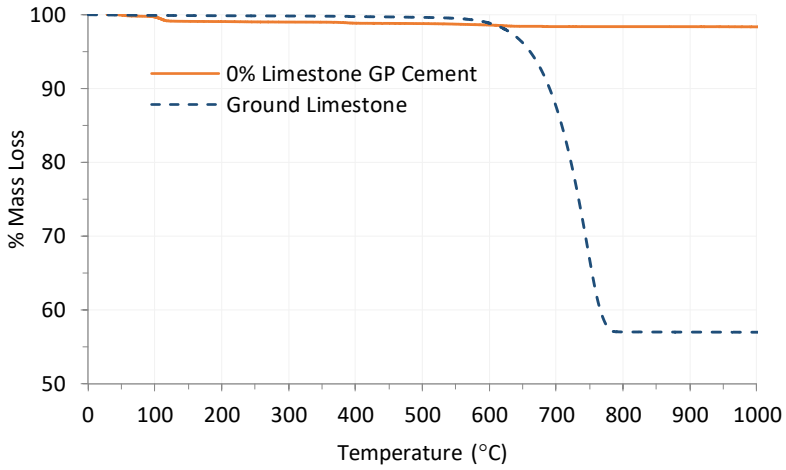

Fig.2. TG Curves of the GP cement and ground limestone

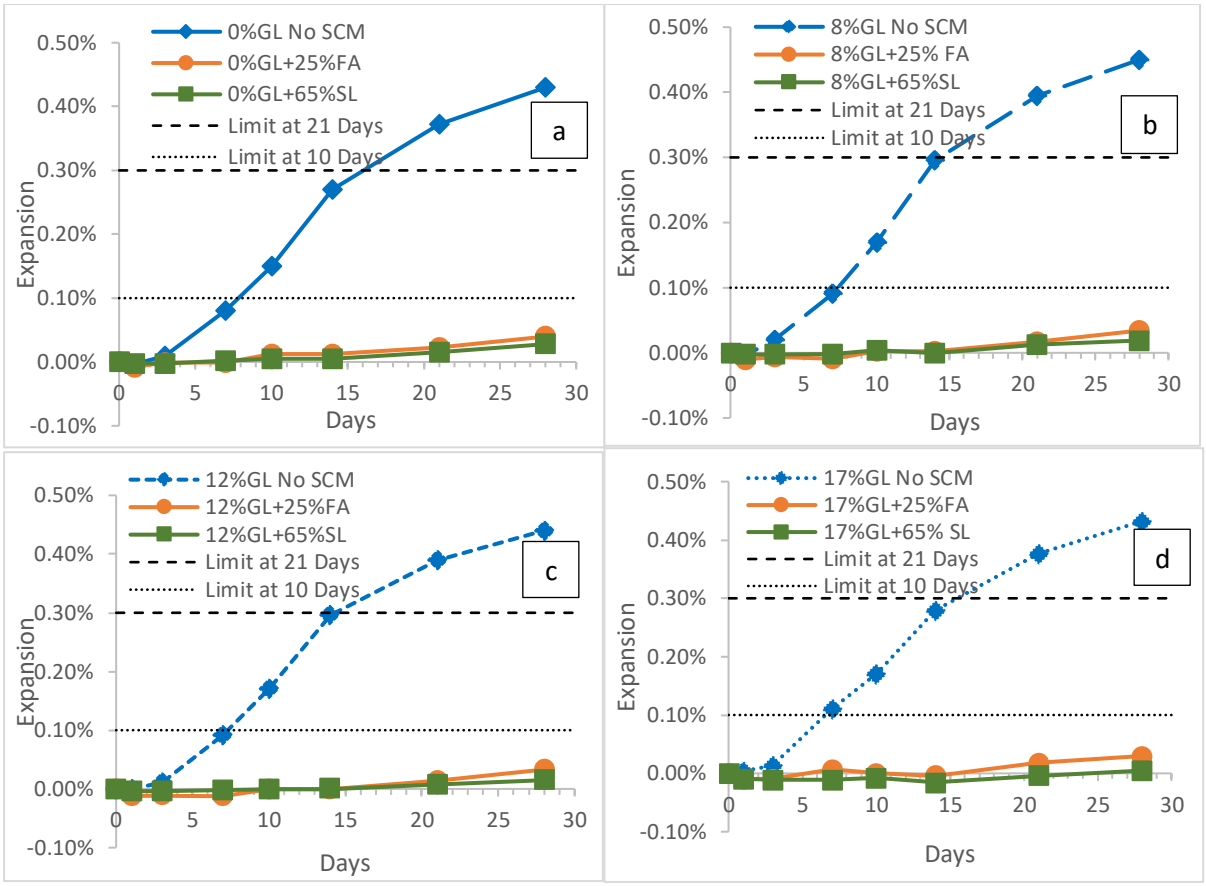

667

668
669

670 **Fig.3.** AMBT expansion results showing effect of SCM addition in binder systems with different limestone

671 contents: a) 0% limestone b) 8% limestone, c) 12% limestone and d) 17% limestone

672

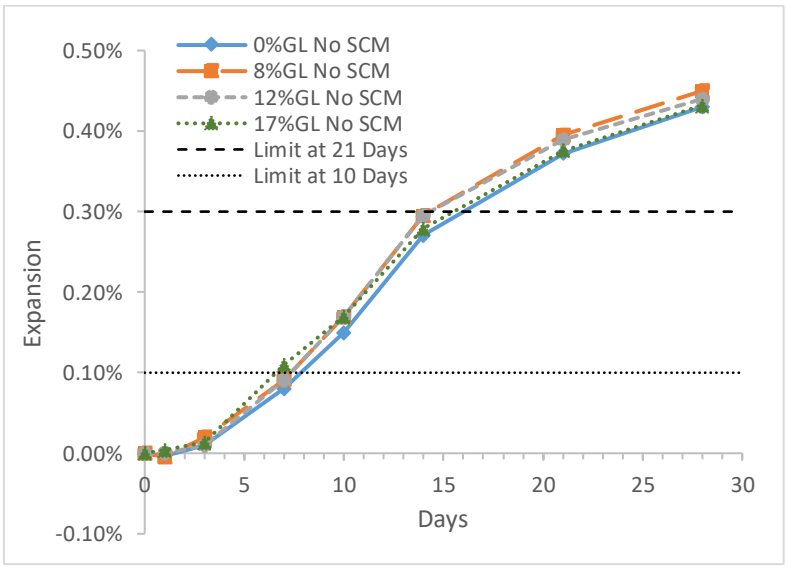

673

674 **Fig.4.** AMBT expansion results of the mortars without SCM showing the effect of cement limestone

675 substitution from 0 to 17%

676

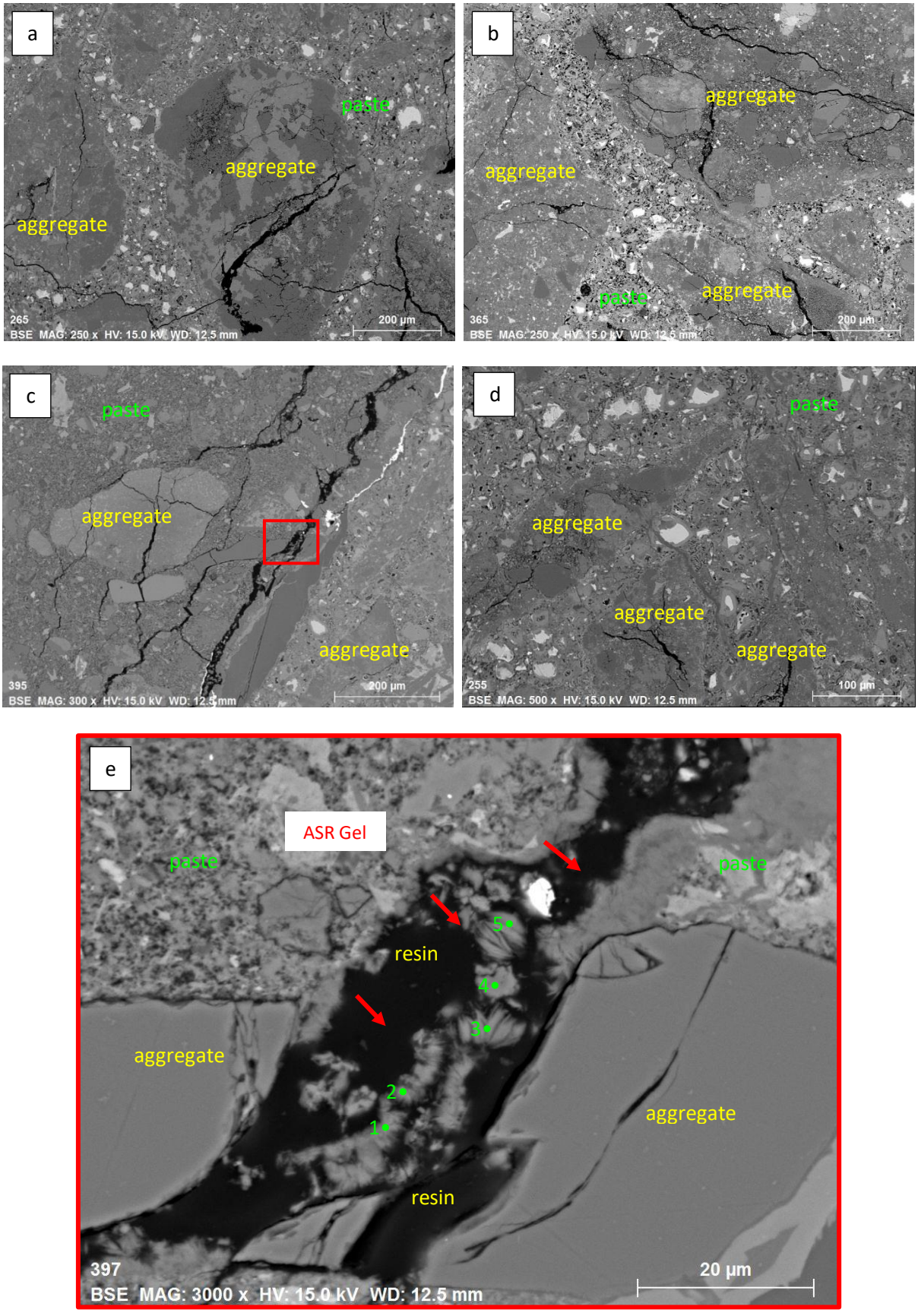

Fig.5. ASR Gel in greywacke mortar without SCM addition a) 0% GL, b) 8% GL, c) 12% GL, d) 17% GL and e) higher magnification image of ASR gel in 12% GL mortar

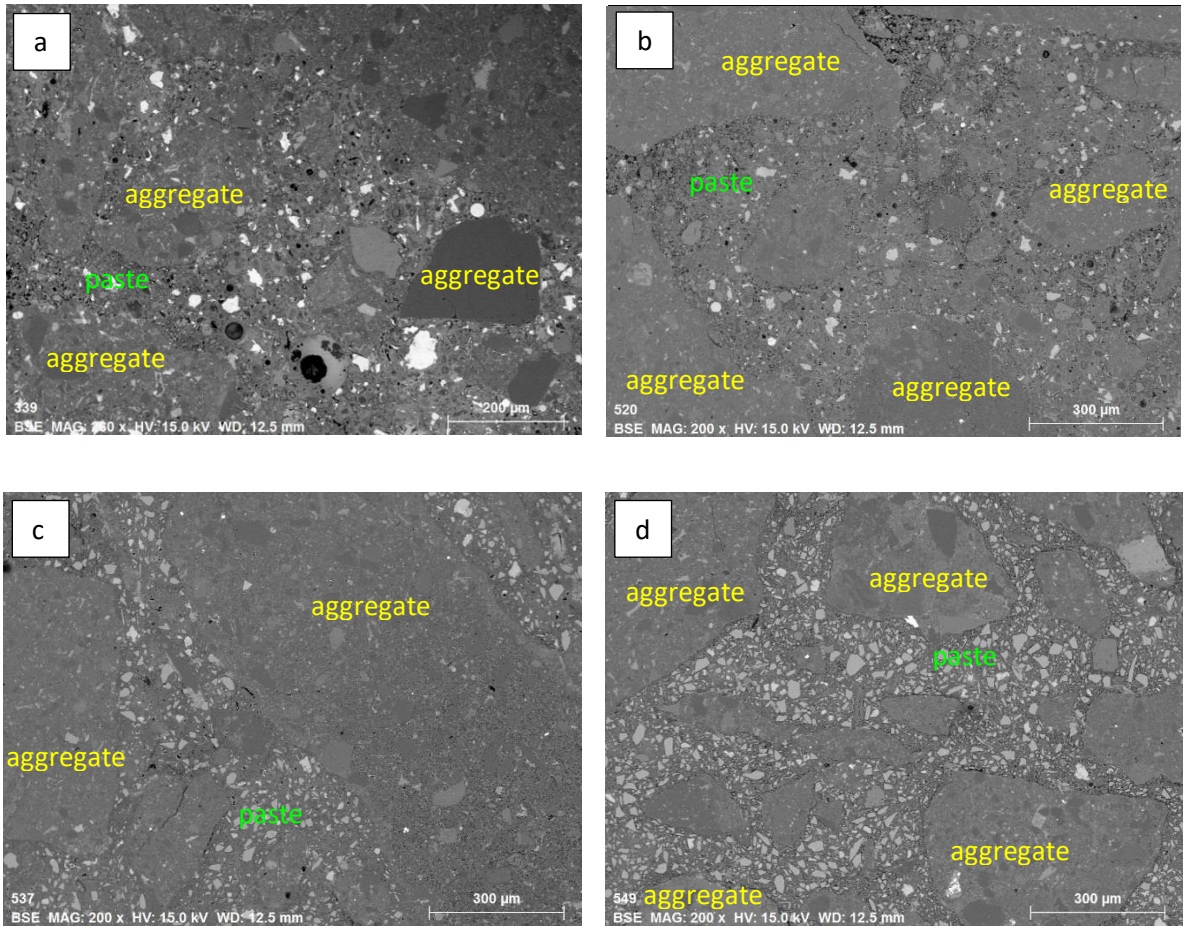

Fig.6. SEM image of the mortars a) 0%GL+ 25%FA, b) 17%GL +25%FA, c) 0%GL+65%SL and d) 17%GL+65%SL

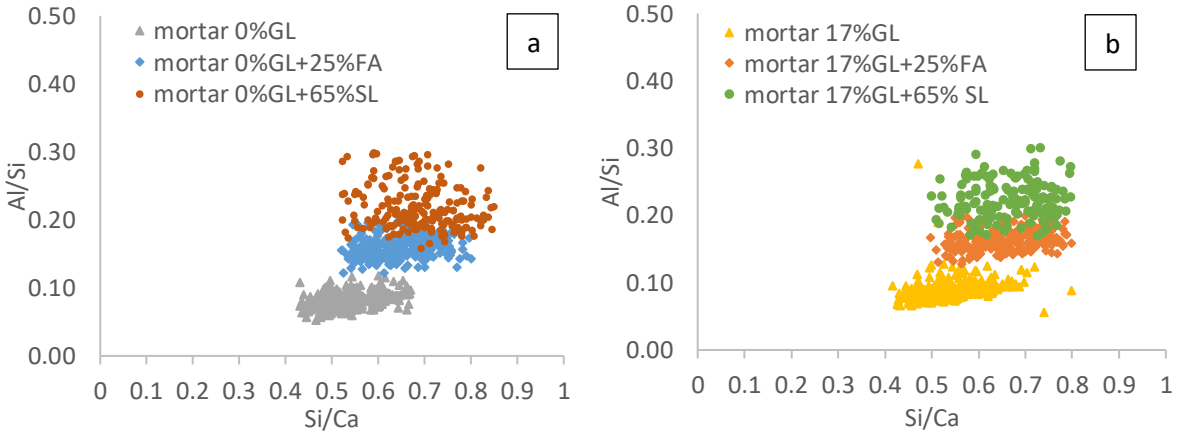

Fig.7. Effect of limestone content on Si/Ca and Al/Si ratio for mortars with a) 0%GL and b) 17%GL

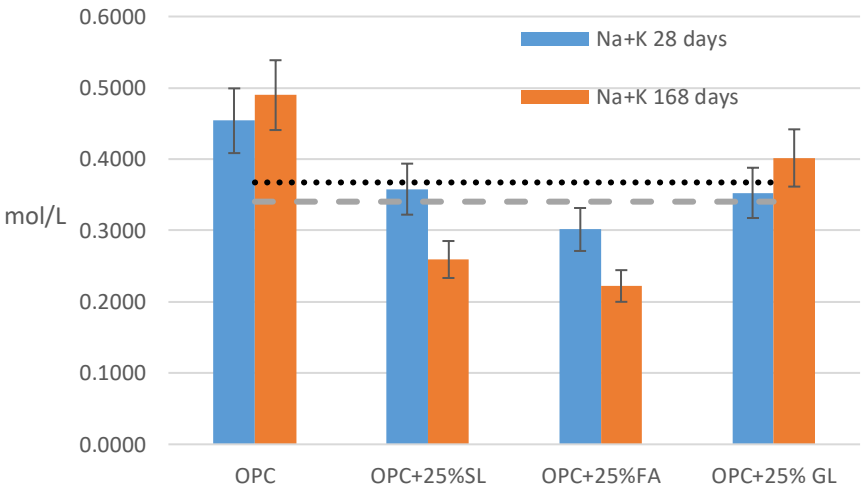

Fig.8. Effect of limestone, fly ash and slag on the pore solution alkali concentration

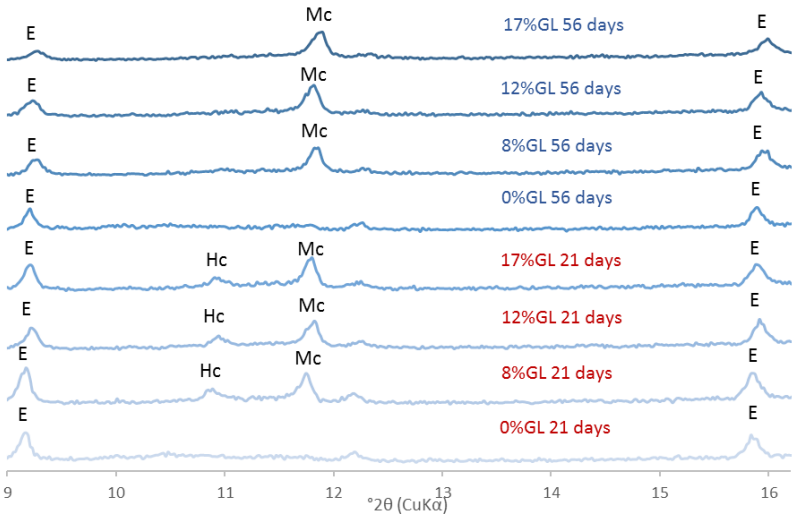

Fig.9. XRD patterns of limestone blended cement pastes without SCMs after 21 days and 56 days ageing at 90%RH, 23±2 °C where E=ettringite, Hc= hemicarboaluminate and Mc=monocarboaluminate.

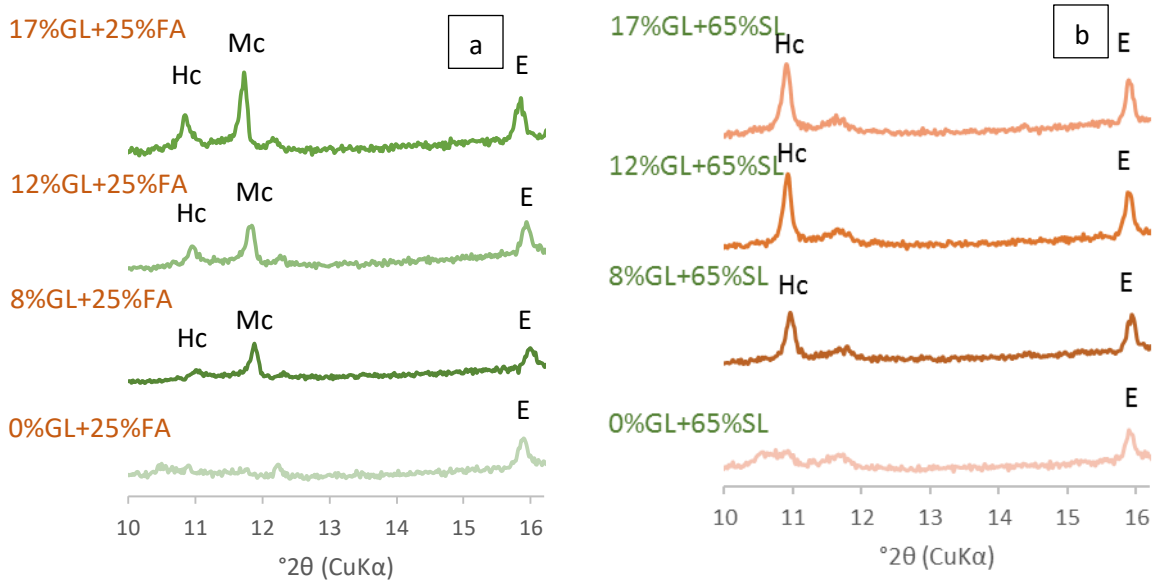

Fig.10. XRD patterns of a) 25% fly ash and b) 65% slag limestone blended cement pastes after 21 days ageing at 90%RH, 23±2 °C where E=ettringite, Hc= hemicarboaluminate, and Mc=monocarboaluminate.

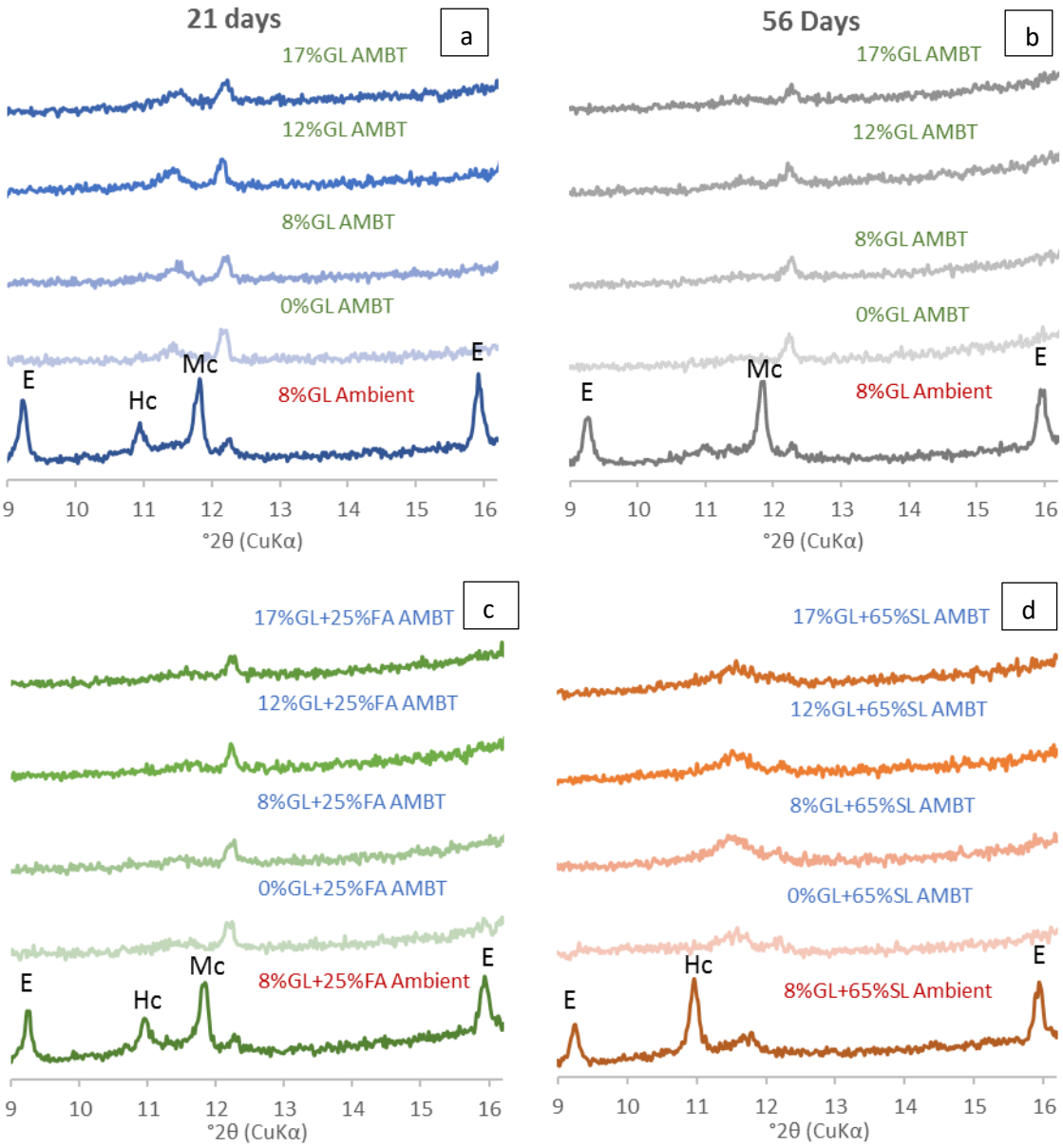

Fig.11. Effect of AMBT conditions (1M NaOH 80 °C) on ettringites and carboaluminates for: a) cement paste at 21 days, b) cement paste at 56 days, c) cement-fly ash-limestone at 21 days and b) cement-slag-limestone pastes at 21 days

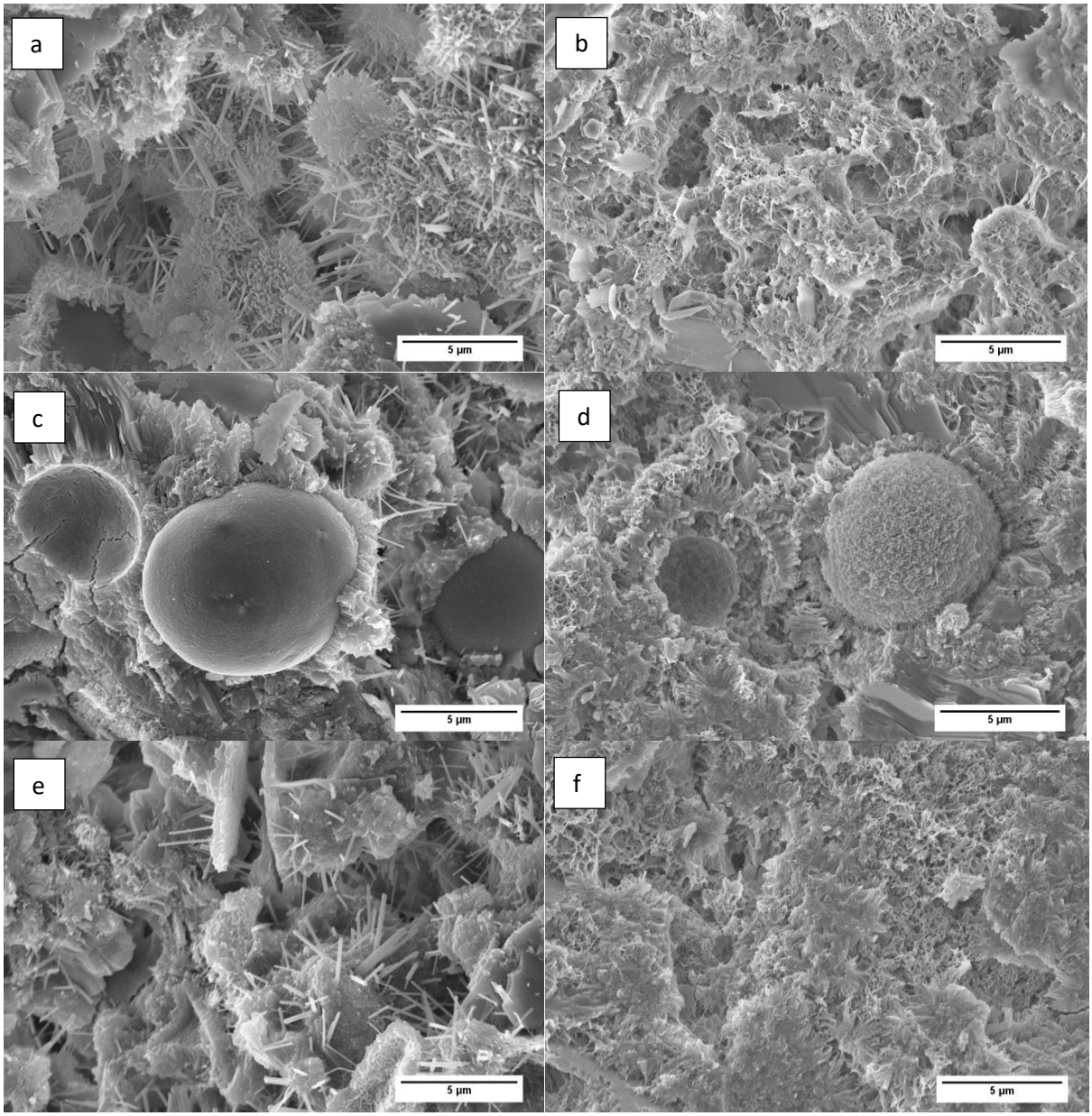

Fig.12. SEM images of cement+ 8%GL without SCM after 21 days a) 90%RH 23±2 °C curing and b) exposure to AMBT conditions (1M NaOH 80 °C), cement+8%GL+25% FA after 21 days c) 90%RH 23±2 °C curing and d) exposure to AMBT conditions (1M NaOH 80 °C) and cement+8%GL+65% SL after 21 days e) 90%RH 23±2 °C curing f) exposure to AMBT conditions (1M NaOH 80 °C).